# Initial nucleation and growth of atomic layer deposited $HfO_2$ gate dielectric layers on Si surfaces with the various surface conditions using *in situ* medium energy ion scattering analysis

K. B. Chung and C. N. Whang
*Institute of Physics and Applied Physics, Yonsei University, Seoul 120-749, Korea*

H. S. Chang, D. W. Moon, and M.-H. Cho[a)]
*Advanced Industrial Technology Group, Korea Research Institute of Standards and Science, Daejeon 305-600, Korea*

(Received 12 July 2006; accepted 1 November 2006; published 3 January 2007)

The initial nucleation and growth of atomic layer deposited $HfO_2$ films under various surface conditions were investigated by *in situ* medium energy ion scattering analysis. The influences of an O–H terminated surface on the initial growth stage were investigated in detail using the atomic density of Hf that reacted on the surface. The measured growth rate of $HfO_2$ per cycle was applied to a mathematical model based on classical chemical kinetics. A parabolic initial growth with an extremely low rate at the initial stage of growth was observed for the film with a hydrogen-terminated surface. However, linear growth, with a value of $1.41 \times 10^{14}$ Hf atoms/cm$^2$ cycle, was maintained for films grown on an O–H terminated surface. The $\sim 1/6$ steric hindrance factor extracted from a phenomenological model was related to the size of the tetrahedral $HfCl_4$ molecule and the possible attachment sites. Moreover, the surface roughness and electrical properties of the atomic layer deposited $HfO_2$ films show a strong dependence on the initial nucleation and growth on the different surface conditions. © *2007 American Vacuum Society.* [DOI: 10.1116/1.2402155]

## I. INTRODUCTION

The reduction of device sizes in the microelectronics industry requires a $SiO_2$ gate dielectric layer thickness smaller than 1.5 nm.[1,2] However, the leakage current is excessive in this regime, leading to a degradation in device performance arising from the direct tunneling current through the thin $SiO_2$ layer.[3,4] As a result, alternative higher dielectric gate oxides have been investigated because high dielectric oxides enable this limitation to be reduced, while still using the same equivalent oxide thickness.[5–7] Among the many potential high dielectric oxides, a $HfO_2$ based high dielectric oxide has attracted considerable attention as a replacement for $SiO_2$ owing to its high dielectric constant ($\sim 20$) and thermodynamic stability on Si.[8–10]

Atomic layer deposition (ALD) is a very promising manufacturing technique for the growth of high-$k$ materials because it is capable of producing high quality films with precise thickness control and uniform conformability.[11,12] For the successful application of a gate oxide using ALD, it is necessary to produce two dimensionally uniform films. Therefore, it is very important to understand the mechanism of ALD growth and to apply a growth model based on experimental results. A number of attempts have recently been made to explain the ALD growth mode, especially the various regimes involved, such as the initial region, the transition region, and the linear region as a function of the number of reaction cycles.[13–16] However, these models employ a number of complicated parameters, thus making an interpretation of the overall process difficult. Puurunen and Vandervorst[16] discussed the restricted growth mode in relation to an island growth. Alam and Green[15] and Green *et al.*[17] also reported on a good mathematical description and its application to a real data set of atomic layer deposited $HfO_2$ using fully *ex situ* Rutherford backscattering (RBS) measurements. Kimura *et al.* reported that high-resolution RBS is a very powerful tool for atomic level characterization for depth resolution at the subnanometer level.[18] Although the reported RBS data give the quantitative quantity for the deposited $HfO_2$, it does not include full information on the earliest growth stage from cycle 1 to cycle 5 due to the effect of surface contamination on the *ex situ* measurements. The ALD growth mode strongly depends on the initial surface reaction prior to the complete deposition of $\sim 1$ ML. The detailed understanding of the earliest growth stage is very important because the properties of dielectric layer depend on the initial control of quality in film and interface.

In this article, we report on the initial growth stage for various surface conditions as a function of the number of deposition cycles using *in situ* medium energy ion scattering (MEIS) analysis. With the aid of a previously reported phenomenological model,[15] very precise measurement data obtained by *in situ* MEIS are used to assign the physical meaning to each of the parameters. The effects on the morphological and electrical characteristics are also discussed in connection with the different growth mechanisms, depending on the surface condition.

[a)]Author to whom correspondence should be addressed; electronic mail: mhcho@kriss.re.kr

## II. EXPERIMENT

*p*-type Si(100) wafers were prepared with two different surface conditions: a chemical oxide surface and a hydrogen-terminated surface. The Si surfaces were chemically cleaned using the standard reduced calcium aluminate method, which removes organic and metallic residues, resulting in the formation of a 10–20 Å thick $SiO_2$ layer.[19] After the RCA cleaning, Si wafers were then dipped in a dilute HF solution to remove the $SiO_2$ layer. $HfO_2$ films were grown using an ALD, equipped with a hot wall reactor with a showerhead. $HfO_2$ films were grown using $HfCl_4$ and $H_2O$ as precursors at a substrate temperature of 300 °C. The temperature of $HfCl_4$ was controlled at 170 °C and $H_2O$ at 14.5 °C. The $N_2$ gas was used as the flow and purge gases. The process pressure for the feeding time was maintained at 250 mTorr. One cycle of ALD-$HfO_2$ growth was consisted of an 800 ms pulse of $HfCl_4$ and a 200 ms pulse of $H_2O$. Each sequence was separated by a $N_2$ purge and a vacuum purge for 100 s to minimize the residual gas reactions, such as the chemical-vapor deposition mode. Two gas lines for the final feeding were used to prevent possible interference.

In order to investigate the initial growth of atomic layer deposited $HfO_2$ films, samples were transferred to an *in situ* MEIS chamber after each ALD deposition cycle. A MEIS analysis using the medium energy ion beam (~100 keV) is unique and permits thin films to be quantitatively examined with a high depth resolution of ~3 Å.[20] Moreover, an *in situ* MEIS analysis can exclude some problems associated with an *ex situ* measurement analysis, such as surface contamination and modification. The MEIS measurement was accomplished with a 100 keV proton ion beam in the double alignment condition, which eliminates contributions from crystalline Si substrates. The incident beams were aligned in the [111] direction and the scattered beams were along the [001] direction with a scattering angle of 125°. During the MEIS measurement, an ion beam with a small area of $5\times10^{-3}$ $cm^2$ was used to scan the wide sample surface and the dose of proton beam was maintained below $\sim10^{15}$ $cm^{-2}$ to minimize damage caused by concentrated hitting. The surface morphology at the initial growth stage of the grown film was examined by means of atomic force microscopy (AFM). A capacitance-voltage (*C-V*) measurement was performed with an HP4284A *LCR* meter at 1 MHz and current-voltage (*I-V*) characteristics were determined with an HP4145B parameter analyzer. A Pt square electrode with an area of about $30\times30$ $\mu m^2$ was patterned by a photolithography process. Finally, interfacial and structural characteristics were investigated by high-resolution transmission electron microscopy (HRTEM).

## III. RESULTS AND DISCUSSION

Figure 1 shows a proton backscattering energy spectra of Hf atoms for $HfO_2$ films grown on the H-terminated surface. The change in Hf peaks represents an increase in Hf coverage with very slow growth rates. An ideal 1 ML spectrum is derived from the simple calculation as the amorphous $HfO_2$ molecular density ($\sim2.49\times10^{22}$ Hf atoms/$cm^3$) to the 2/3

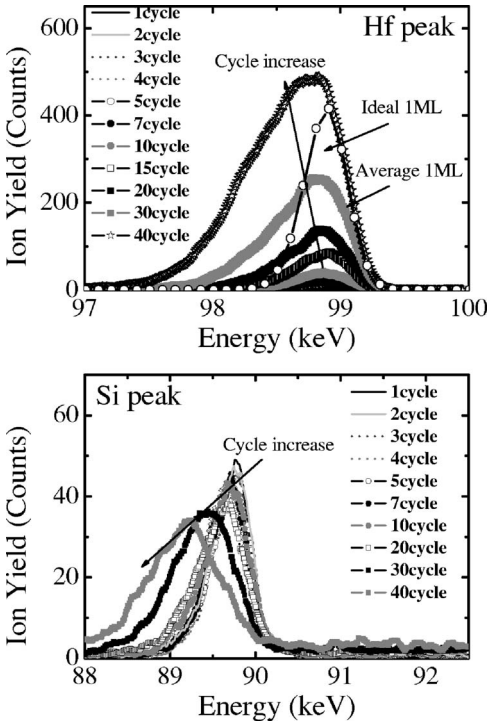


FIG. 1. MEIS energy spectra of $HfO_2$ grown on the H-terminated surface with increasing number of $HfO_2$ deposition cycles. Arrows indicate that the ideal, average 1 ML (at 30 cycles), and the direction of cycle increased, respectively.

power, equal to $8.53\times10^{14}$ Hf atoms/$cm^2$. The Hf peak of ~30 cycles, corresponding to the ideal 1 ML coverage, has a remarkably broad peak. Therefore, the growth of $HfO_2$ on the H-terminated surface deviates substantially from the general linear growth at the initial stage. Moreover, the lower slope in the Hf peak compared to that of an ideal Hf peak implies that $HfO_2$ grown on the H-terminated surface has a poor morphology due to the contribution of nonlinear growth. In addition, the movement of the Si leading edge provides information on the $HfO_2$ growth behavior on a Si substrate because the effective blocking of the underlying Si is directly related to the number of Hf atoms on the Si surface. If Hf fully covers the Si and films have no roughness factor, shift of the leading edge of the Si signal should move backward because of the effective blocking by the fully covered Hf.[21] However, no movement in the Si leading edge was observed for a low energy at ~30 cycles, when an average Hf coverage of 1 ML is achieved. This implies that the Si surface is incompletely covered with the $HfO_2$ film. In other words, the growth of $HfO_2$ films has the roughness factor, not perfect ALD growth. The slopes of the Si peak decrease substantially with increasing deposition cycles, also indicating that the surface of $HfO_2$ films has a nonuniform morphology. Another interesting finding is that we were not able to observe evidence for the formation of interfacial layer such as a silicate. If the interfacial layer was formed at the initial growth stage of $HfO_2$, a small shoulder related to the interface should be observed at the near leading edge of the Si peak. The Si shoulder in the MEIS spectrum is related to the

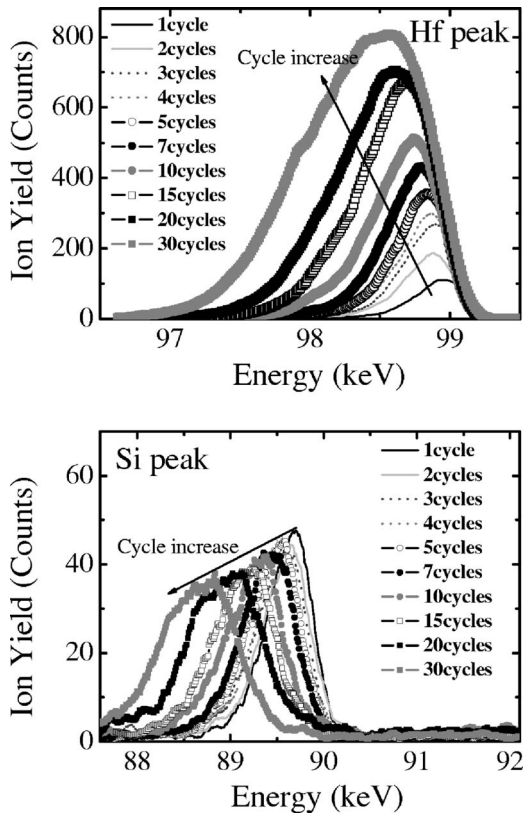


FIG. 2. MEIS energy spectra of $HfO_2$ grown on a chemical oxide surface with increasing number of $HfO_2$ deposition cycles.

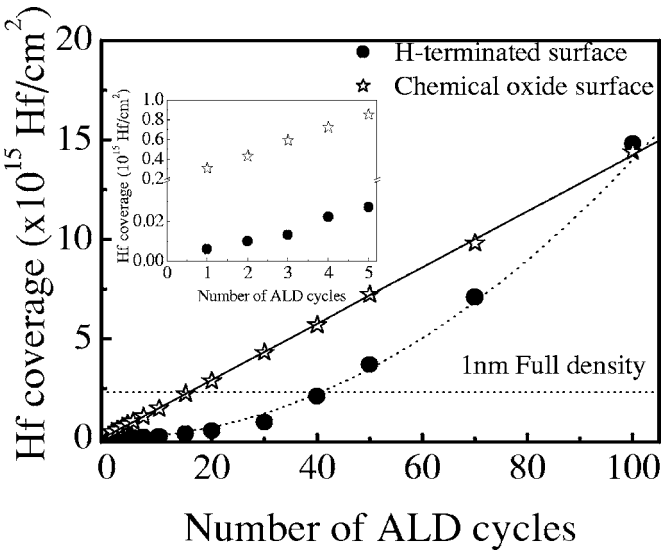


FIG. 3. Hf coverage, measured by *in situ* MEIS, as a function of the number of $HfO_2$ deposition cycles, for the H-terminated surface and the chemical oxide surface. A parallel dotted line indicates a 1 nm full density of $HfO_2$. Hf coverage at the earliest stage is shown in the inset. The fitting data are included to a solid line ($k_1N_0=1.41\times10^{14}$ Hf/cm$^2$) for linear fitting and a dotted line ($k_2=0.003$) for parabolic fitting.

formation of silicate or not fully covered Si substrate because the Si peak can be differentiated from that of the Si substrate covered by the film. However, it was difficult to find this feature from our MEIS results on the Si peak for the H-terminated surface. This could be due to one of the following two reasons. One is that the H-terminated surface is very stable at a growth temperature of 300 °C and interfacial reactions are suppressed on the surface.[22] Second, as we previously reported, silicate in the interface region is slightly formed on the thermal oxide, as evidenced by the x-ray photoelectron spectroscopy study, though no meaningful information could be obtained from MEIS measurements.[21] Thus, it is reasonable that the formation of the interfacial layer is very slight during $HfO_2$ growth on the H-terminated surface in the resolution limit of MEIS. On the other hand, the Hf peak for $HfO_2$ grown on the chemical oxide surface exhibits a linear increment for Hf coverage: i.e., the growth behavior of the film shows a linear and rapid growth rate, compared to $HfO_2$ growth on the H-terminated surface, as shown in Fig. 2. The slopes of the Hf peak do not change significantly with an increase in the number of $HfO_2$ deposition cycles, implying a uniform and flat morphology. At the same time, the fact that the Si peaks gradually move backward without a change in the shape as the deposition cycles increase also supports the linear growth behavior.

For a more detailed interpretation of the $HfO_2$ growth mechanism, the MEIS spectra of the Hf peak were simulated using the KIDO program.[23] Figure 3 shows a plot of Hf coverage, as measured by *in situ* MEIS, as a function of the number of $HfO_2$ deposition cycles, for the H-terminated surface and the chemical oxide surface. Extremely different growth behaviors are observed: the growth on the H-terminated surface is nonlinear and the growth on the chemical oxide surface is linear. The parallel dotted line representing 1 nm of density is based on ~90% density ($\sim2.49\times10^{15}$ Hf atoms/cm$^2$ nm) of the theoretical crystalline molecular density ($2.77\times10^{15}$ Hf atoms/cm$^2$ nm) because the deposited $HfO_2$ films with an amorphous structure have a lower density than that with a crystalline structure. In the case of the H-terminated surface, a large nonlinear growth with a very slow growth rate at the initial stage is observed (up to ~30 cycles), which can be explained by a nucleation hindrance effect. In a practical situation in ALD growth, an incubation period at the initial growth stage is observed, which would be closely related to this nonlinear growth. However, the growth behavior on the chemical oxide shows linear characteristics even in the earliest deposition cycles, indicating that growth on the chemical oxide surface has no nucleation barriers, contrary to that of the H-terminated surface. The inset of Fig. 3 shows more detailed behaviors at the earliest growth stage. A noteworthy point is that the Hf coverage at 1 cycle is strikingly different between $HfO_2$ films grown on the chemical oxide and the H-terminated surface. The coverage of growth on the chemical oxide surface at 1 cycle is $\sim3.1\times10^{14}$ Hf atoms/cm$^2$ and that on the H-terminated surface is $\sim5.7\times10^{12}$ Hf atoms/cm$^2$. From this large discrepancy of about two orders in possible attachment sites, it appears that the earliest nucleation of $HfO_2$ is dominantly affected by the initial surface conditions. The two extremely different growth behaviors depending on the surface conditions can be

interpreted as follows. The H-terminated surface is very stable and contains a low density of OH species, whereas the chemical oxide surface is known to have a high density of OH species.[22] Accurate measurements of Si–OH densities have been carried out only on $SiO_2$ surfaces and found to be in the range of $(1-7)\times10^{14}$ OH/cm$^2$ depending on the surface pretreatments.[24] The OH density on the chemical oxide surface is most likely at the level of $\sim7\times10^{14}$ OH/cm$^2$. The difference in OH density affects the initial nucleation behavior, resulting either in linear or nonlinear growth. Therefore, the presence of OH species is very important to the nucleation and growth of ALD $HfO_2$ using a halide precursor.[25] The value of the slope of the linear fitting to the Hf coverage on the chemical oxide shown in the Fig. 3 is calculated to be $1.41\times10^{14}$ Hf atoms/cm$^2$ cycle. This value is minutely different from data in a previous report in which *ex situ* RBS measurements were used.[17] The maximum $HfO_2$ area l density of 1 ML was already extracted as $8.53\times10^{14}$ Hf atoms/cm$^2$. Thus, only $\sim$16% area is covered with $HfO_2$ molecules per cycle above 2 cycles, and more than six deposition cycles are needed to for the entire surface to be covered, considering the reaction of Si–OH nucleation site at the initial stage. This implies that growth on the chemical oxide surface is also a partially monolayer growth per cycle and has the typical value for the steric hindrance ($\sim1/6$), which is in good agreement with the calculated value of the adsorbed molecular size using a tetrahedral $HfCl_4$ molecule structure.[26]

The Hf coverage data fitted to the solid line and dotted line are also included in Fig. 3. We used a previously reported phenomenological model based on the classical chemical kinetic theory, from which two differential equations are derived.[15] One describes the deposition rate per cycle of $HfO_2$, and the other the rate of creation of OH sites (Si–OH and Hf–OH) per cycle. The major assumptions are that the half reactions are allowed to proceed to saturation that no desorption of adsorbed species occurs during the purge steps, and OH species (Si–OH and Hf–OH) are nucleation sites for ALD growth using halide precursors such as $HfCl_4$.[25,27] In the case of growth on the H-terminated surface, a parabolic solution can be obtained by approximating the following parameters: $N_{\text{init}} \ll N_0$, $K_{\text{cov}}=1$.

$$N_{\text{HfO}_2} = N_{\text{init}}C + \left(\frac{k_2}{2}\right)(N_0 - N_{\text{init}})C^2, \tag{1}$$

where $N_{\text{HfO}_2}$ is the amount of $HfO_2$, $K_{\text{cov}}$ is the OH site utilization factor as a function of $HfO_2$ coverage, $N_{\text{OH}}$ is the net number of potential nucleation sites, $k_2$ is the rate constant for the creation of Si–OH nucleation sites, and $N_0$ is the number of potential nucleation sites ($=8.53\times10^{14}$ cm$^{-2}$). If the first term of Eq. (1) (because $N_{\text{init}}$ is initially almost zero) is abbreviated, the experimental data can be matched with the parabolic solution, which has the fitted parameter $k_2=\sim0.003$, as shown in Fig. 3. The physical meaning of this is that about 3 out of 1000 potential nucleation sites are converted to Si–OH sites per cycle. Therefore, initially, growth on the H-terminated surface has a very slow deposition rate. To consider the growth on the chemical oxide surface, the parameters can be approximated with the following values: $N_{\text{init}}\sim N_0$, $K_{\text{cov}}=k_1$ (since the OH sites are closed packed, $K_{\text{cov}}$ has the constant $k_1$, the sterically hindered value),

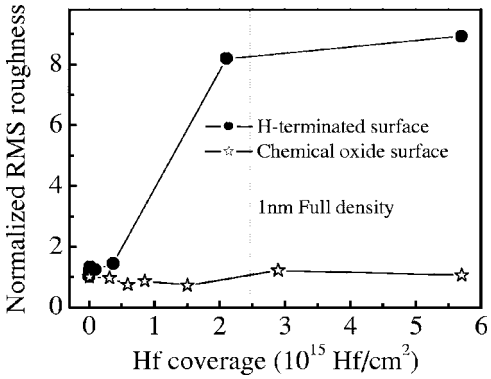


FIG. 4. Normalized AFM measurements of $HfO_2$ films grown on the H-terminated surface and the chemical oxide surface as a function of $HfO_2$ coverage.

$$N_{\text{HfO}_2} = k_1 N_0 C. \tag{2}$$

The solution has the characteristics of linear growth behavior, which are in accord with the experimental data. The slope in Fig. 3 is the $k_1N_0=1.41\times10^{14}$ Hf/cm$^2$, from which we can obtain the steric hindrance factor $k_1=\sim1/6$. Considering the size of the incoming $HfCl_4$ molecules,[26] the result value is reasonable because the steric hindrance factor means the screening effects for absorption of a $HfCl_4$ molecule due to previously absorbed $HfCl_4$ molecules. Finally, we can conclude that the initial growth on the H-terminated surface and on the chemical oxide surface are parabolic and linear, respectively, through the application of *in situ* MEIS data with the help of the simplified phenomenological growth model.

Figure 4 shows the AFM data normalized to the roughness of each starting surface. The results show that the H-terminated surface case is rougher than the chemical oxide surface case. Rough and islandlike growth occurred in the case of the H-terminated surface growth, while growth on the chemical oxide surface preserved a smooth surface as the $HfO_2$ coverage increases. These tendencies as a function of $HfO_2$ coverage are consistent with the characteristics of the MEIS spectra shown in Figs. 1 and 2 as a function of the number of cycles. In other words, a disturbance in the initial nucleation on the H-terminated surface results in the rough surface of $HfO_2$ layer such as a three-dimensional island structure. The expansion of surface area available for reaction due to the roughness may cause an increase in deposition rate after the initial growth stage. In addition, it is possible that the morphology of rough surface generates the growth of porous films for the same $HfO_2$ coverage.[28] Therefore, the lower density of $HfO_2$ films can be affected by the rough surface of $HfO_2$ films grown on the H-terminated surface, which is caused by the nonlinear growth mode in the initial regime.

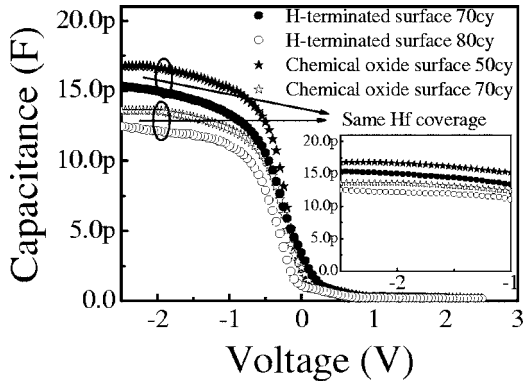


FIG. 5. *C-V* curves of $HfO_2$ films grown on the H-terminated surface and the chemical oxide surface: the Hf coverage of 70 and 80 cycles on the H-terminated surface is the same as that for 50 and 70 cycles on the chemical oxide surface, respectively. The inset shows the expanded region around −2−−1 V.

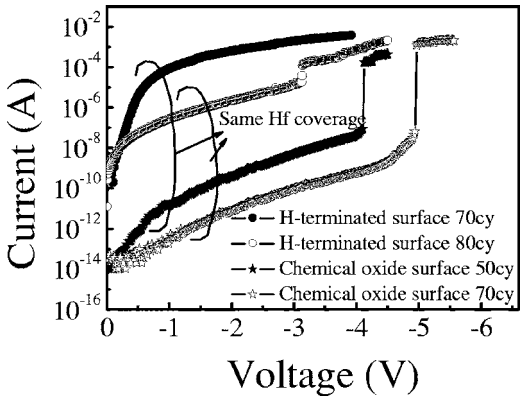


FIG. 6. *I-V* characteristics of $HfO_2$ films grown on the H-terminated surface and the chemical oxide: the Hf coverage of 70 and 80 cycles on the H-terminated surface is the same as that for 50 and 70 cycles on the chemical oxide surface, respectively.

In order to investigate the electrical characteristics in relation to the initial nucleation and growth of $HfO_2$ films, capacitance-voltage (*C-V*) and current-voltage (*I-V*) were measured as a function of the number of deposition cycles. A metal-oxide-semiconductor structure was prepared with a Pt gate electrode area of $30\times30$ $\mu m^2$ by using the photolithography process. Figure 5 shows the typical *C-V* curves of $HfO_2$ films grown on the H-terminated surface and the chemical oxide surface. The Hf coverage of 70 deposition cycles and the 80 cycles on the H-terminated surface are equal to that of 50 deposition cycles and the 70 cycles on the chemical oxide surface, respectively, as determined by the MEIS results shown in Fig. 3. The $HfO_2$ films grown on the H-terminated surface have a smaller accumulation capacitance than that on the chemical oxide surface for the same Hf coverage. The difference in accumulation capacitance could be due to the following two effects. One is that the 1–2 nm $SiO_2$ layer for $HfO_2$ films grown on the chemical oxide surface affects the decrease in accumulation capacitance. The other is that the difference in the density of $HfO_2$ films contributes to the accumulation capacitance. If the density of $HfO_2$ films depending on the initial surface conditions is excluded, the accumulation capacitance of $HfO_2$ grown on the chemical oxide should be less than that of $HfO_2$ grown on the H-terminated surface due to the serial connection of the $SiO_2$ layer with the thickness of 1–2 nm. However, our results show the inverse tendency, i.e., that the accumulation capacitance of $HfO_2$ films grown on chemical oxide is higher than the films on a H-terminated surface. As compared with the previous MEIS results of the $HfO_2$ films grown on chemical oxide and on H-terminated surface with the same Hf coverage (e.g., 10 cycles for the chemical oxide and 40 cycles for H-terminated surface with 1 nm full density of $HfO_2$), we found that the height and width of the Hf peak show a discrepancy. $HfO_2$ films grown on chemical oxide have a higher height and the narrower width for the Hf peak. This means that the $HfO_2$ films grown on chemical oxide have a higher film density than the films on the H-terminated surface. In addition, a larger roughness makes the film more porous: i.e., the densification of films is relatively low, which effects the electrical thickness. Generally, the dielectric constant ($\varepsilon$) has been explained by the Clausius-Mosotti formula as a function of polarizability ($\alpha$).[29] Polarizability ($\alpha$) is related to the molar volume ($V_m$), which is proportional to the capacitance.[30] Therefore, the difference in the density of $HfO_2$ films depending on the initial growth and the relative decrease of molar volume due to its relatively low density can be attributed to a reduction in the accumulation capacitance of films grown on the H-terminated surface.

Figure 6 shows the *I-V* characteristics of $HfO_2$ films grown on a H-terminated surface and on a chemical oxide surface, respectively. The leakage current is increased by about four orders of magnitude for $HfO_2$ films grown on the H-terminated surface for almost all deposition cycles, compared with the films on the chemical oxide surface. In addition to the leakage current, the breakdown voltage is increased in $HfO_2$ films grown on the chemical oxide surface, compared with the films on the H-terminated surface with the same Hf coverage. This is obviously related to differences in the interface prior to the growth of the films on the two different Si surfaces, as shown in the previous *C-V* data. Because the interfacial oxide such as the chemical oxide of $SiO_2$ acts as another insulator in the $HfO_2$ film, compared to the films grown on the H-terminated film, the leakage current is relatively decreased. Nevertheless, another most important thing is that the density of $HfO_2$ films caused by the difference of the ALD growth mode depending on the surface conditions, such as the layered growth on the chemical oxide surface, influences the electrical properties.

In order to better understand the relationships between leakage current characteristics and the surface conditions, the MEIS results and HRTEM images are considered, as shown in Figs. 7 and 8.[31] Figure 7 shows (a) MEIS energy spectra and (b) compositional depth profiles for 70 deposition cycles on the H-terminated surface and 50 cycles on the chemical oxide surface with the same Hf coverage, respectively. From the width of the O peak, the total thickness is the same for $HfO_2$ films grown on the under different surface conditions.

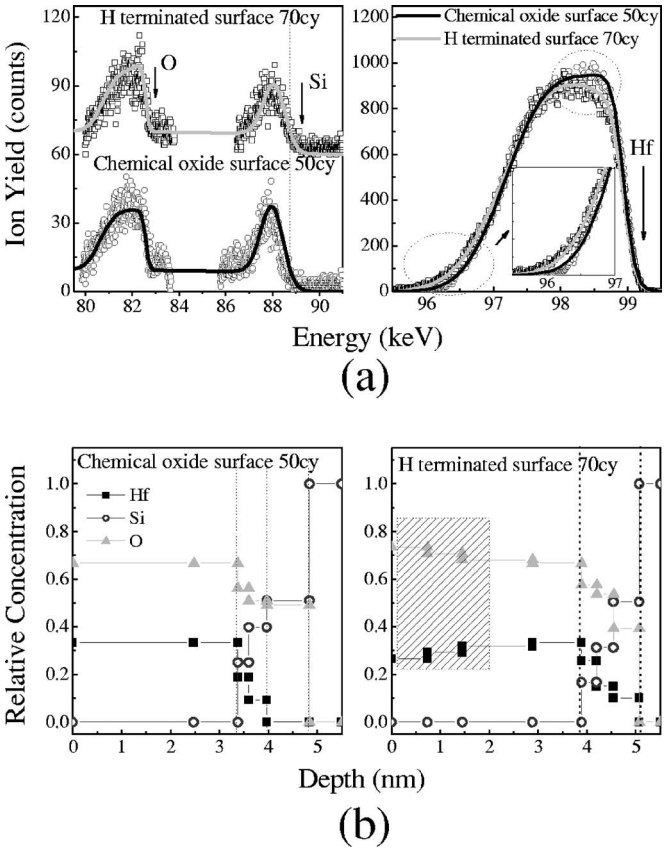


FIG. 7. (a) MEIS energy spectra and (b) compositional depth profiles for 70 cycles on the H-terminated surface and 50 cycles on the chemical oxide surface with the same Hf coverage. Inset in (a) indicates the enlargement of interfacial region in Hf peak. The hatched region in (b) represents a nonuniform distribution of concentration for $HfO_2$ films grown on the H-terminated surface.

However, the amount of Hf distributed is different in the Hf region, as indicated by dotted circles. The amounts of Hf grown on the chemical oxide surface are higher than that on the H-terminated surface in the surface region. On the contrary, the quantities of Hf grown on the chemical oxide surface are lower than that on the H-terminated surface in the interfacial region. In addition, $HfO_2$ films on the chemical oxide surface have a sharp interface as evidenced by the steep slope of the Hf peak, as shown in the inset. These results are in agreement with the compositional depth profiles calculated from the simulation via the KIDO program in Fig. 7(b). The $HfO_2$ films grown on the chemical oxide surface have a uniformly distributed concentration throughout the entire films and an abrupt interface. On the other hand, $HfO_2$ films grown on the H-terminated surface have a nonuniform concentration in the surface region up to a thickness of ~2 nm, as indicated by the hatched region. In order to assess the MEIS interpretations, HRTEM images were investigated for 60 deposition cycles on the H-terminated surface and 50 cycles on the chemical oxide surface. Even if the thickness of the $HfO_2$ films has a discrepancy because of the difference of deposition cycles in the case of films on the H-terminated surface, the HRTEM results show that the $HfO_2$ films have a different uniformity of film density depending on the surface conditions. $HfO_2$ films grown on the chemical oxide surface have a uniform density distribution, however, those on the H-terminated surface have a nonuniform density distribution and rough surface morphology, which is consistent with the AFM data. Therefore, the difference in the density distribution of $HfO_2$ films caused by the different ALD growth modes depending on the surface conditions is strongly related to the electrical characteristics.

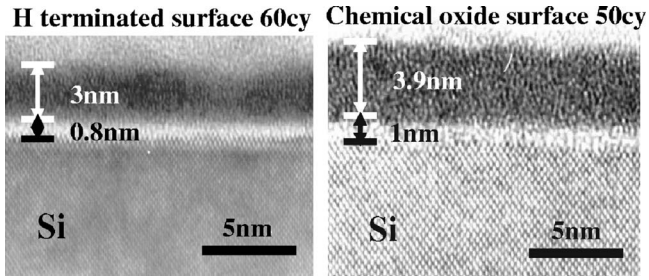


FIG. 8. HRTEM images after 60 cycles on the H-terminated surface and 50 cycles the chemical oxide surface.

## IV. CONCLUSION

The initial nucleation and growth of atomic layer deposited $HfO_2$ films were examined using *in situ* MEIS analysis. The growth on the H-terminated surface was compared to the results obtained for a chemical oxide surface. These were applied to a simplified mathematical model related to the nucleation sites of a $HfCl_4$ molecule. Parabolic initial growth occurs on the H-terminated surface with an ~0.003 creation rate to nucleation sites for a $HfCl_4$ molecule. The chemical oxide enables $HfO_2$ nucleation with a linear growth rate with a value of $1.41 \times 10^{14}$ Hf atoms/cm$^2$ and an ~1/6 steric hindrance factor. $HfO_2$ films grown on the chemical oxide surface with a linear growth rate lead to smooth morphology and superior electrical properties.

## ACKNOWLEDGMENT

This work was supported by the National Program for Tera-level Nanodevices of the Ministry of Science and Technology as one of the 21 Century Frontier Programs.

[1]M. L. Green, E. P. Gusev, R. Degraeve, and E. L. Garfunkel, J. Appl. Phys. **90**, 2057 (2001).
[2]Semiconductor Industry Association, The International Technology Roadmap for Semiconductors.
[3]D. A. Muller, T. W. Sorsch, S. Moccio, F. H. Baumann, K. Evans-Lutterodt, and G. Timp, Nature (London) **399**, 758 (1999).
[4]H. Fukuda, M. Yasuda, and T. Iwabuchi, Appl. Phys. Lett. **61**, 693 (1992).
[5]K. J. Hubbard and D. G. Schlom, J. Mater. Res. **11**, 2757 (1996).
[6]G. D. Wilk, R. M. Wallace, and J. M. Anthony, J. Appl. Phys. **89**, 5243 (2001).
[7]Angus I. Kingon, Jon-Paul Maria, and S. K. Steriffer, Nature (London) **406**, 1032 (2000).
[8]M.-Y. Ho *et al.*, Appl. Phys. Lett. **81**, 4218 (2002).
[9]G. D. Wilk, R. M. Wallace, and J. M. Anthony, J. Appl. Phys. **87**, 484 (2000).
[10]M.-H. Cho *et al.*, Appl. Phys. Lett. **81**, 472 (2002).
[11]T. Suntola, Mater. Sci. Rep. **4**, 261 (1989).
[12]M. Ritala, K. Kukli, A. Rahtu, P. I. Räisänen, M. Leskelä, T. Sajavaara,

and J. Keinonen, Science **288**, 319 (2000).
[13]H.-S. Park, J.-S. Min, J.-W. Lim, and S.-W. Kang, Appl. Surf. Sci. **158**, 81 (2000).
[14]A. Satta *et al.*, J. Appl. Phys. **92**, 7641 (2002).
[15]M. A. Alam and M. L. Green, J. Appl. Phys. **94**, 3403 (2003).
[16]R. L. Puurunen and W. Vandervorst, J. Appl. Phys. **96**, 7686 (2004).
[17]M. L. Green *et al.*, J. Appl. Phys. **92**, 7168 (2002).
[18]K. Kimura, S. Joumori, Y. Oota, K. Nakajima, and M. Suzuki, Nucl. Instrum. Methods Phys. Res. B **219–220**, 351 (2004).
[19]W. Keren, RCA Rev. **31**, 207 (1970).
[20]E. P. Gusev, H. C. Lu, T. Gustafsson, and E. Garfunkel, Phys. Rev. B **52**, 1759 (1995).
[21]H. S. Chang, H. Hwang, M.-H. Cho, and D. W. Moon, Appl. Phys. Lett. **86**, 031906 (2005).
[22]H. Ikeda, K. Hotta, T. Yamada, S. Zaima, H. Iwano, and Y. Yasuda, J. Appl. Phys. **77**, 5125 (1995).
[23]Y. Kido and T. Koshikwa, J. Appl. Phys. **67**, 187 (1990).
[24]S. Haukka and T. Suntola, Interface Sci. **5**, 119 (1985).
[25]T. Suntola, Appl. Surf. Sci. **100/101**, 391 (1996).
[26]M. Yliammi, Thin Solid Films **279**, 124 (1996).
[27]S. M. Georgem, A. W. Ott, and J. W. Klaus, J. Phys. Chem. **100**, 13121 (1996).
[28]S.-K. Song, S.-K. Koh, D. Y. Lee, K. M. Song, and H.-K. Baik, Jpn. J. Appl. Phys. Part 1 **43**, 6452 (2004).
[29]C. Kittel, *Introduction to Solid State Physics* (Wiley, New York, 1996).
[30]R. D. Shannon, J. Appl. Phys. **73**, 348 (1993).
[31]K. B. Chung, H. S. Chang, S. H. Lee, C. N. Whang, D.-H. Ko, H. Kim, D. W. Moon, and M.-H. Cho, Electrochem. Solid-State Lett. **8**, F51 (2005).